Photosynthetic adaptation to low iron, light, and temperature in Southern Ocean phytoplankton

Robert F. Strzepek[a,1], Philip W. Boyd[a,b], and William G. Sunda[c]

[a]Antarctic Climate and Ecosystems Cooperative Research Centre, University of Tasmania, Hobart, TAS 7001, Australia; [b]Institute for Marine and Antarctic Studies, University of Tasmania, Hobart, TAS 7001, Australia; and [c]Department of Marine Sciences, University of North Carolina at Chapel Hill, Chapel Hill, NC 27599

Edited by David M. Karl, University of Hawaii, Honolulu, HI, and approved January 23, 2019 (received for review June 25, 2018)

Phytoplankton productivity in the polar Southern Ocean (SO) plays an important role in the transfer of carbon from the atmosphere to the ocean's interior, a process called the biological carbon pump, which helps regulate global climate. SO productivity in turn is limited by low iron, light, and temperature, which restrict the efficiency of the carbon pump. Iron and light can colimit productivity due to the high iron content of the photosynthetic photosystems and the need for increased photosystems for low-light acclimation in many phytoplankton. Here we show that SO phytoplankton have evolved critical adaptations to enhance photosynthetic rates under the joint constraints of low iron, light, and temperature. Under growth-limiting iron and light levels, three SO species had up to sixfold higher photosynthetic rates per photosystem II and similar or higher rates per mol of photosynthetic iron than temperate species, despite their lower growth temperature (3 vs. 18 °C) and light intensity (30 vs. 40 μmol quanta·m^{2}·s^{-1}), which should have decreased photosynthetic rates. These unexpectedly high rates in the SO species are partly explained by their unusually large photosynthetic antennae, which are among the largest ever recorded in marine phytoplankton. Large antennae are disadvantageous at low light intensities because they increase excitation energy loss as heat, but this loss may be mitigated by the low SO temperatures. Such adaptations point to higher SO production rates than environmental conditions should otherwise permit, with implications for regional ecology and biogeochemistry.

iron | light | temperature | Southern Ocean | phytoplankton

Marine microscopic phytoplankton are responsible for half of global photosynthesis (1). They form the base of the marine food web and transfer carbon from the atmosphere to the ocean's interior, a process called the biological carbon pump. Carbon fixation by Southern Ocean (SO) phytoplankton plays a particularly important role in the efficiency of the ocean's carbon pump and hence regulation of atmospheric carbon dioxide (CO_2) (2, 3). Iron (Fe) limits photosynthetic carbon fixation in ~30% of the ocean and is particularly limiting in the frigid waters of the SO, where light availability and low temperature also restrict phytoplankton growth and productivity (3–5).

The SO possesses distinct flora, fauna, and ecosystems due to its unique environmental conditions and geographical isolation (6, 7). Such isolation raises other key scientific issues, such as how life evolved in this polar region, and how it has successfully subsisted under the harshest of marine conditions (7). There is emerging genomic evidence of unprecedented isolation of phytoplankton communities in the SO over sufficiently long timescales for directional selection to take place (8). If we are to predict how such isolated populations will fare in a rapidly changing ocean, we need to first understand how these primary producers adapted to the three major environmental factors that limit primary productivity in the SO—low iron supply, low temperatures, and low underwater light levels (4). The recent focus on the role of iron in limiting SO productivity (3, 5) has obscured a physiological enigma—if resident phytoplankton acclimate to low light as most temperate species do, by increasing the number of iron-rich photosystems (9), this would exacerbate iron limitation (10–13). SO phytoplankton could resolve this dilemma by increasing the size (pigment content) of their photosystems to increase light absorption (14). However, large increases in antenna size decrease the fraction of absorbed light energy transferred to reaction centers, which can be disadvantageous under limiting light conditions (14–17).

To examine this adaptation, experiments were conducted with iron-sufficient and iron-limited cultures of three bloom-forming SO phytoplankton: the diatoms *Eucampia antarctica* and *Proboscia inermis* and the haptophyte *Phaeocystis antarctica*. Results from these experiments were compared with those for two well-studied temperate diatoms: *Thalassiosira weissflogii* and *Thalassiosira oceanica*, isolated respectively from high-iron coastal and low-iron oceanic waters. The SO and temperate species were grown at representative temperatures for their environments (3 and 18 °C). They were cultured at low light intensities (30 and 40 μmol quanta·m^{-2}·s^{-1}, respectively, for the SO and temperate species), which limited growth rates by 21 ± 5% and 35 ± 10% (±SE) relative to light-saturating rates (18). The lower light intensity was needed in the SO species to achieve light limitation of specific growth rate at the low 3 °C growth temperature (18).

The temperate oceanic species is able to grow at much lower iron concentrations than the coastal species due to a lower cellular iron requirement for growth, which has been attributed to a much lower ratio of iron-rich photosystem I (PSI) to lower iron photosystem II (PSII) (13). The SO species also can grow at exceptionally low intracellular iron levels (18, 19), but the mechanisms responsible for this ability have not been examined in detail. Here we report measurements of the cellular content of

Significance

Controls on phytoplankton productivity in the extreme environment of the Southern Ocean has received widespread attention. This polar region presents three challenges to primary producers: how to subsist under the joint constraints of low temperatures, low light, and growth-limiting concentrations of the essential trace element iron. The resident phytoplankton have overcome these extreme environmental conditions with a unique combination of physiological adaptations. They have modified parts of their photosynthetic machinery to harvest low levels of light without substantially increasing their iron requirements, and in a way that may exploit the low temperature in their environment. Together, these adaptations enable them to use iron and light more efficiently and grow faster than environmental conditions should otherwise permit.

Author contributions: R.F.S. and P.W.B. designed research; R.F.S. performed research; R.F.S. and W.G.S. analyzed data; and R.F.S., P.W.B., and W.G.S. wrote the paper.

The authors declare no conflict of interest.

This article is a PNAS Direct Submission.

[1]To whom correspondence should be addressed. Email: robert.strzepek@utas.edu.au.

This article contains supporting information online at www.pnas.org/lookup/suppl/doi:10.1073/pnas.1810886116/-/DCSupplemental.

Table 1. Relationships among specific growth rate, photosynthetic Fe-to-C ratios, and photosynthetic iron use efficiencies in SO species (grown at 3 °C) and in temperate oceanic and coastal diatoms (grown at 18 °C)

Species	Region	Iron level	Growth rate, d^{-1}	Fe_{PH}:C, $\mu mol \cdot mol^{-1}$	PS IUE, kmol C·mol $Fe_{PH}^{-1} \cdot d^{-1}$	PSII:PSI
P. inermis	SO	Low	0.30 ± 0.01	2.1 ± 0.5	143 ± 33	2.0 ± 0.4
		High	0.44 ± 0.01	3.5 ± 0.7	127 ± 27	0.8 ± 0.2
E. antarctica	SO	Low	0.14 ± 0.02	1.6 ± 0.4	87 ± 26	1.3 ± 0.3
		High	0.26 ± 0.01	1.6 ± 0.5	163 ± 47	2.4 ± 0.4
P. antarctica	SO	Low	0.15 ± 0.00	1.1 ± 0.2	131 ± 27	1.8 ± 0.2
		High	0.33 ± 0.04	4.6 ± 2.2	72 ± 36	1.4 ± 0.3
T. oceanica	Temperate Oceanic	Low	0.38 ± 0.01	2.8 ± 0.8	137 ± 41	7.5 ± 2.1
		High	0.67 ± 0.03	6.4 ± 1.1	105 ± 19	10.8 ± 1.6
T. weissflogii	Temperate Coastal	Low	0.34 ± 0.01	9.5 ± 0.9	36 ± 4	4.4 ± 0.4
		High	0.55 ± 0.01	20.9 ± 3.2	26 ± 4	1.7 ± 0.2

Fe_{PH}, photosynthetic Fe; PS IUE, photosynthetic iron use efficiencies.

the two photosystems (PSI and PSII), normalized to cell carbon, in iron-limited and iron-sufficient SO algal species, which we compare with those in the temperate diatoms. These measurements are of significance because the photosystems constitute the core of the photosynthetic apparatus and, along with the cytochrome b_6f complex, represent the main iron-containing components in phytoplankton (10, 13). From measurements of cellular photosystem and carbon content, chlorophyll *a* (Chl *a*), specific growth rates, and rates of photosynthetic O_2 evolution, we were able to compute photosynthetic rates and Chl *a* content per photosystem in the iron-limited and iron-replete SO species and the two temperate diatoms.

Results

The specific growth rates of the iron-limited cultures were reduced by 32 to 55% relative to those in the iron-sufficient cultures (Table 1; $P < 0.05$, *SI Appendix*, Table S4). Cellular PSI and PSII normalized to cell carbon (C) differed among the species, especially between the SO and temperate ones and the temperate coastal and oceanic diatoms (Fig. 1 *C* and *D*). In general, photosystem:C ratios were lower in the iron-limited cultures, consistent with their lower specific growth rates (Fig. 1 *C* and *D*; $P < 0.05$, *SI Appendix*, Table S5). Under iron limitation, PSI:C ratios in the SO species were similar to that in the temperate oceanic diatom, but were fivefold lower on average than in the temperate coastal diatom (Fig. 1*D*; $P < 0.05$, *SI Appendix*, Table S5). PSII:C ratios were up to 10-fold higher in the temperate diatoms than in the SO species (Fig. 1*C*; $P < 0.05$, *SI Appendix*, Table S5).

PSII:PSI ratios also differed among the SO and temperate species (Table 1; $P < 0.05$, *SI Appendix*, Table S4). The mean PSII:PSI ratio in the iron-limited and iron-sufficient SO species (1.7 ± 0.2) (±SE) equaled that (1.7) for the iron-sufficient coastal diatom *T. weissflogii*, but was lower than that (4.4) for this same species grown under iron limitation or those for the oceanic temperate diatom *T. oceanica* grown under iron limitation (7.5) and sufficiency (10.8) (Table 1).

The maximum photosynthetic oxygen (O_2) evolution rates normalized to Chl *a* (P^B_{max}) of the iron-limited cultures were reduced by 1.3-fold in *T. oceanica* ($P > 0.05$), 1.7-fold in *T. weissflogii* ($P < 0.05$), and 2.1-fold in the SO species ($P < 0.05$) relative to those in the iron-sufficient cultures (*SI Appendix*, Fig. S1 and Table S2; ANOVA, *SI Appendix*, Table S6). P^B_{max} of the three SO species was lower than that in the temperate species under both iron sufficiency and iron limitation, likely reflecting the lower growth temperature of the SO species (*SI Appendix*, Table S2; $P < 0.05$, *SI Appendix*, Table S6). The maximum (light-saturated) photosynthetic electron transport rates ($1/\tau$; ms^{-1}) from water to a terminal electron acceptor [assumed to be principally CO_2 (14)] were 2.4 ± 0.5 and 2.7 ± 0.4 (±SE) times faster, respectively, in iron-limited and iron-sufficient SO species than in the temperate diatoms (Fig. 2*E*; $P < 0.05$, *SI Appendix*, Table S7). Dark respiration rates were significantly lower in the SO species than in the temperate diatoms (Fig. 2*F*; $P < 0.05$, *SI Appendix*, Table S7).

The initial slope of the photosynthesis–irradiance (P–E) curve, α^B, increased ~2.7-fold under iron limitation in the SO species ($P < 0.05$) and *T. weissflogii* ($P > 0.05$) but decreased 2.6-fold ($P < 0.05$) in *T. oceanica* [Fig. 3 and *SI Appendix*, Table S2; Tukey's multiple comparison test (MCT), *SI Appendix*, Table S6]. α^B is the product of the in vivo absorption cross-section normalized to Chl *a* (a*) and the quantum yield of photosynthesis (φ_m). Thus, the 2.7-fold increase in α^B in the iron-limited SO species may indicate an increase in the quantum yield, but may also partly be caused by a 22 to 57% decrease in Chl *a* per unit of cell surface area (*SI Appendix*, Table S1) and resulting decrease in Chl self-shading (20). An increase in

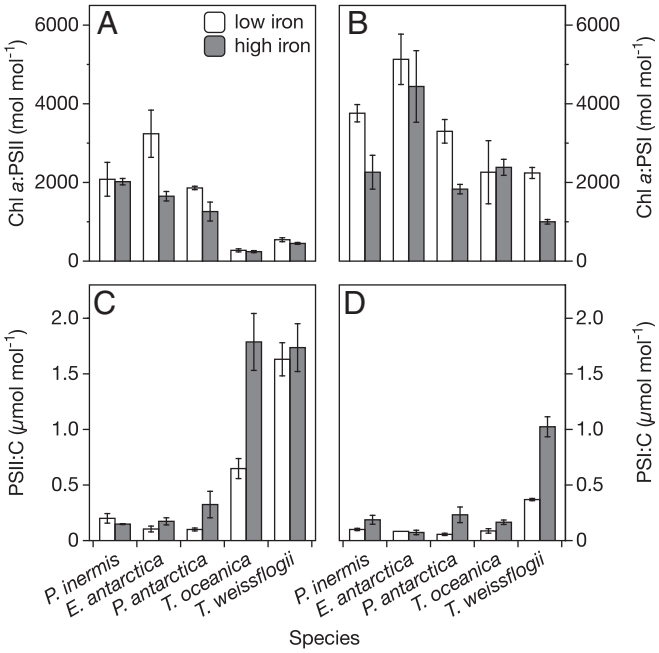

Fig. 1. Ratios of cellular Chl *a* to PSII (*A*), cellular Chl *a* to PSI (*B*), PSII to cell C (*C*), and PSI to cell C (*D*) in low-iron (open bars) and high-iron (shaded bars) SO and temperate phytoplankton species. Error bars represent the SE of replicate cultures, and are smaller than the symbols when not visible ($n = 3$ to 9).

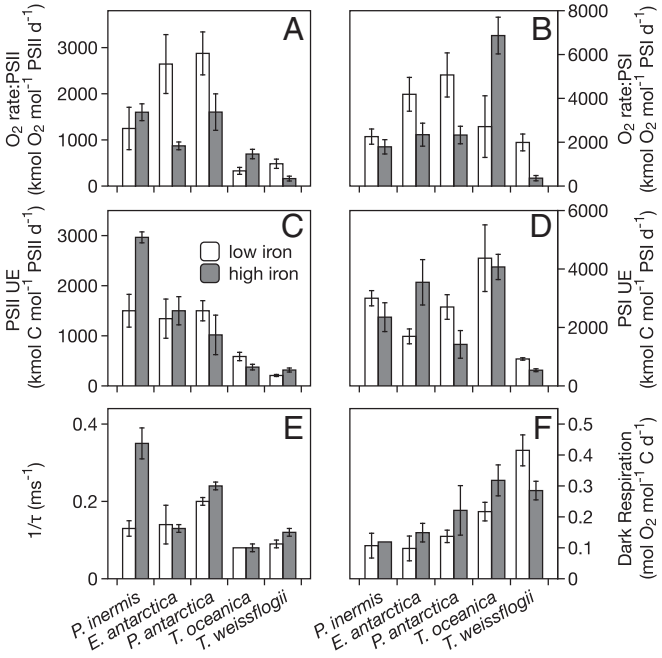

Fig. 2. Gross O_2 production rates per PSII (*A*) and PSI (*B*); PSII (*C*) and PSI (*D*) use efficiencies (UEs); maximum steady-state electron turnover rates from water to CO_2 (*E*); and dark respiration rates normalized to cell C (*F*) in low-iron (open bars) and high-iron (shaded bars) SO and temperate phytoplankton species. Error bars represent the SE of replicate cultures, and are smaller than symbols when not visible (n = 3 to 9).

α^B under iron limitation has been observed previously with O_2-based measurements of photosynthesis (20), but not with the short-term (hours) ^{14}C-based method (21–23). The difference in the results of the two methods may be linked to the fact that the short-term ^{14}C method measures neither gross nor net C-fixation rates, while the O_2 method measures rates of photosynthetic O_2 production minus O_2 consumption from respiration and photorespiration, which may be lessened under iron and light limitation (24, 25).

Measurements of specific growth rates, photosynthetic O_2 evolution rates, and PSI:C and PSII:C ratios allowed us to assess the photosynthetic efficiency of the two photosystems. Using the P–E relationships (Fig. 3), we estimated O_2 photoproduction rates and O_2 PS use efficiencies for all species at 30 μmol quanta·m^{-2}·s^{-1}, the growth irradiance of the SO species, but not of the temperate species, which, as noted earlier, were grown at a higher light intensity (40 μmol quanta·m^{-2}·s^{-1}) to obtain a more comparable degree of light limitation between the two sets of species. This increase in light intensity increased photosynthetic O_2 production rates by 29% on average in the temperate species (Fig. 3 and *SI Appendix*, Fig. S1). In iron-limited cultures, the mean O_2 PSII use efficiency of the SO species was, respectively, 4.7- and 6.9-fold higher than in the temperate coastal and oceanic diatoms (Fig. 2*A* and *SI Appendix*, Table S3; $P < 0.05$). For iron-limited cultures, the mean O_2 PSI use efficiency for the SO species was not significantly different from that for the temperate oceanic diatom (Fig. 2*B* and *SI Appendix*, Table S3; $P > 0.05$, Tukey's MCT, *SI Appendix*, Table S7).

Carbon use efficiencies for PSII and PSI were computed by dividing the specific growth rate by the PSII:C and PSI:C ratios, and have units of net mol of fixed C per mol of photosystem per d. In the iron-limited cultures, the C PSII use efficiencies were on average 2.5- and 7.0-fold higher in the SO species than in the temperate oceanic and coastal diatoms, respectively (Fig. 2*C*; $P < 0.05$, *SI Appendix*, Table S7), and the average C PSI use efficiency in the SO species was 2.7-fold higher than in the temperate coastal diatom (Fig. 2*D* and *SI Appendix*, Table S3; $P > 0.05$, *SI Appendix*, Table S7) but 44% lower than in the temperate oceanic diatom ($P > 0.05$).

The PSII:C and PSI:C ratios allowed us to estimate photosynthetic iron:C ratios, and thus photosynthetic iron use efficiencies. In these calculations, we assumed that the amount of cytochrome (Cyt) b_6f complex equaled that of PSI (13) and that Cyt c_6 and ferredoxin, which contain iron, were replaced by the iron-free proteins plastocyanin and flavodoxin (13, 26). We also assumed that PSII and PSI contain 2 and 12 Fe, respectively, while the Cyt b_6f complex contains 5 (10). For the iron-limited cultures, the mean photosynthetic Fe:C ratio in the SO species was 1.62 ± 0.34 (±SE) μmol·mol^{-1}, 1.7- and 5.9-fold less than in the temperate oceanic and coastal diatoms, respectively (Table 1). The photosynthetic Fe:C values equaled 75 ± 18% (±SE) of the previously measured cellular Fe:C ratios (*SI Appendix*, Table S1) in both low- and high-iron cultures of the temperate species and four of the five SO species (all but *P. inermis*), which verifies previous theoretical calculations and observations that the photosynthetic apparatus represents the dominant intracellular iron pool, and hence that iron and light limitation are metabolically linked (10–13). However, for *P. inermis*, the photosynthetic Fe:C ratios were four- to fivefold higher than the measured cellular Fe:C ratios (*SI Appendix*, Table S1), an impossibility if the photosystems and Cyt b_6f complex contain their normal complement of iron. The observed discrepancy is most likely caused by an erroneously low measured intracellular iron value in this large fragile diatom.

Photosynthetic iron use efficiencies were computed by dividing the specific growth rate by the photosynthetic iron concentration (Table 1). The mean use efficiencies for the three SO species were 120.2 ± 20.9 (±SE) kmol C·(mol Fe)$^{-1}$·d^{-1} for the

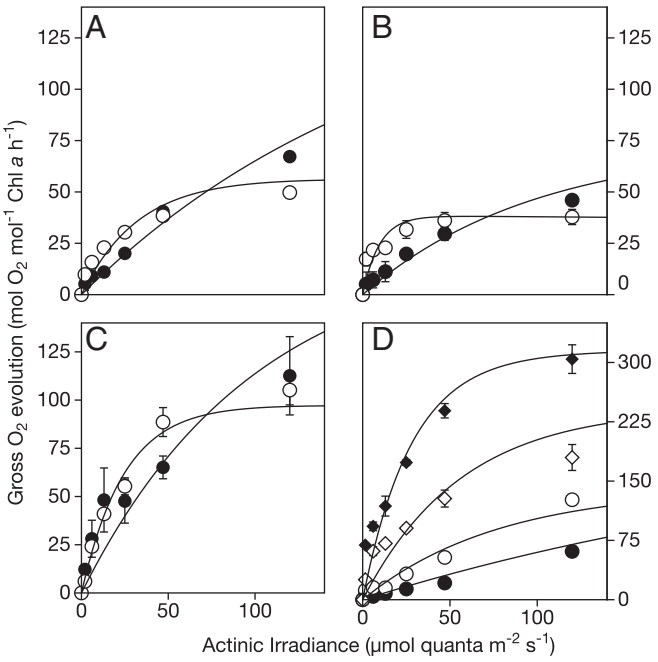

Fig. 3. Photosynthesis-versus-irradiance curves for the light-limited portion of the actinic irradiance range (0 to 140 μmol quanta·m^{-2}·s^{-1}). Mean gross oxygen evolution rates are plotted as a function of actinic irradiance for low-iron (open symbols) and high-iron (closed symbols) cultures. (*A*) *P. inermis*, (*B*) *E. antarctica*, (*C*) *P. antarctica*, and (*D*) *T. oceanica* (diamonds) and *T. weissflogii* (circles). Note the different *y*-axis scale in *D*. Error bars represent the SE of replicate cultures, and are smaller than the symbols when not visible (n = 3). Solid lines denote exponential model fits (47). See *SI Appendix*, Fig. S1 for the full P–E curves, and *SI Appendix*, Table S2 for the photosynthetic parameters derived from the modeled P–E curves.

iron-limited cultures and 120.4 ± 15.5 kmol C·(mol Fe)$^{-1}$·d^{-1} for both the iron-limited and iron-sufficient cultures combined. Similar values ($P > 0.05$) were observed for the temperate oceanic diatom [137.0 and 121.1 kmol C·(mol Fe)$^{-1}$·d^{-1} under iron limitation and combined conditions, respectively]. But the mean SO value was 3.4-fold higher than the value for the temperate coastal diatom under iron limitation, and it was 4.6-fold higher under iron sufficiency (Table 1).

Discussion

The higher C-based photosynthetic iron use efficiencies in the SO species than the temperate coastal species are expected because all three of the SO species are oceanic, and oceanic species have lower iron requirements than coastal ones due to their adaptation to much lower oceanic iron concentrations (27, 28). However, the similarity between C-based use efficiencies for the SO species and the oceanic temperate species is surprising given the higher light intensity (40 vs. 30 μmol photons·m^{-2}·s^{-1}) and temperature (18 vs. 3 °C) for *T. oceanica*, which both should have increased rates of photosynthesis and growth (14). The higher expected rates at the higher temperature result from higher diffusion rates of small photosynthetic electron carriers (plastoquinone, plastocyanin, flavodoxin, and NADPH) and higher reaction rates of the numerous enzymes involved in C fixation and biosynthesis (14).

The unexpectedly high PS use efficiencies and photosynthetic iron use efficiencies in the iron-limited SO species were likely facilitated by higher amounts of Chl *a* per PS and associated higher-functional absorption cross-sections of PSII (σ_{PSII}) and PSI. The Chl *a*:PSII ratios in the iron-limited cultures were on average 4.4- and 8.7-fold higher in the SO species than in the temperate coastal and oceanic species, respectively (Fig. 1*A*), and were associated with 4.7- and 3.0-fold higher σ_{PSII} (Fig. 4; $P < 0.05$, *SI Appendix*, Table S8). These Chl *a*:PSII ratios and σ_{PSII} values were among the highest ever recorded (9, 10, 16, 23).

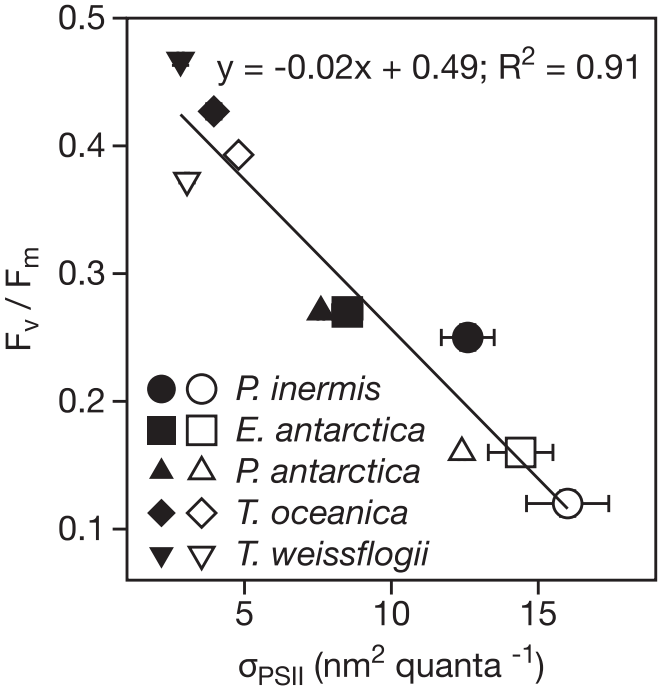

Fig. 4. Inverse correlation between variable-to-maximum PSII fluorescence and the functional absorption cross-section of PSII. Open and closed symbols are for low- and high-iron cultures, respectively. Error bars represent the SE of replicate cultures, and are smaller than the symbols when not visible (n = 3 to 9). The solid line denotes linear regression.

The highest σ_{PSII} values were observed in the two iron-limited SO diatoms, whose volumes per cell (51,300 fL for *P. inermis* and 11,100 fL for *E. antarctica*) were much larger than iron-limited values for *P. antarctica* (16.9 fL) and *T. oceanica* (56 fL) (*SI Appendix*, Table S1). The combination of large cell size and large σ_{PSII} values is surprising, because high-absorption cross-sections have been previously observed only in small-celled species, where the decreased cell size results in increased surface-to-volume ratios and resultant decreases in chlorophyll self-shading (package effects) (14, 16). However, the iron-limited SO diatoms appear to have overcome this adverse effect of large cell size by decreasing their Chl:cell volume ratios by 3.3- to 20-fold and C:cell volume ratios by 6.6- to 46-fold relative to those in the much smaller *P. antarctica* and *T. oceanica* (*SI Appendix*, Table S1). These decreases presumably result from the presence of large cell vacuoles, which commonly occur in large algal cells and can greatly reduce protoplasm-to-cell volume ratios (29).

Large light-harvesting antennae not only cause increased Chl self-shading but also decrease efficiency of transfer of light excitation energy to photosynthetic reaction centers (10, 15, 17), as seen from the strong inverse correlation ($R^2 = 0.91$) between σ_{PSII} and variable-to-maximum fluorescence (F_v/F_m), a measure of the photosynthetic efficiency of PSII (16) (Fig. 4). This photosynthetic inefficiency for absorbed light is disadvantageous at growth-limiting light intensities, but nonetheless appears to have been favored evolutionarily for growth and survival of phytoplankton in the iron- and light-stressed SO. Similar inverse relationships between F_v/F_m and σ_{PSII} have been observed (16), including in SO algal communities growing under varying iron stress levels (30). Under light-saturating conditions, at least some of the low F_v/F_m values in iron-limited phytoplankton appear to result from pigment protein complexes that are disconnected from their PSII reaction centers (30–32), but such disconnected centers would be disadvantageous under the light-limiting conditions of our experiments, as they would increase Chl self-shading.

The low temperature of the SO may facilitate the large pigment antenna sizes of PSII and PSI and mitigate their inherent inefficiencies in light energy transduction. Very large antenna sizes are disadvantageous because they increase residence times of light excitation energy, and thus increase energy loss as heat and fluorescence (10, 15, 17). However, heat loss should decrease with decreasing temperature (15), leaving more available excitation energy to drive photosynthesis. Indeed, polar species are able to grow phototrophically at extremely low light levels (33), and the increased light energy transfer efficiency in photosynthetic antennae at low temperatures may be an important factor in this phenomenon.

In addition, another possible cause for the high SO photosynthetic efficiencies, especially those for PSII, may be the use of proteorhodopsin (PR), whose gene transcripts have been observed in all three of our experimental SO species, but not in *T. oceanica* or other species of the genus *Thalassiosira* (34–36). Transcripts of this protein have been found in phytoplankton communities and isolates from iron-limited waters of the subarctic Pacific (34–36) and SO (26, 34), and its expression is down-regulated with iron addition in field experiments and algal cultures (34–36). Like photosynthesis, PRs absorb light energy to produce a pH gradient across cell membranes, which may be used to produce additional needed ATP over that produced by linear photosynthetic electron transport (PET) (37, 38) (*SI Appendix*, Fig. S2). But, unlike iron-containing photosynthetic proteins, PRs are iron-free, and thus can result in a considerable iron saving to the cell (34).

Other adaptations may also have contributed to the high photosystem use efficiencies and low iron requirements in the SO phytoplankton. These include low rates of the iron-intensive process of respiration (10), normalized to cell C, in the SO species relative to values in *T. oceanica*, and especially

T. weissflogii (Fig. 2*F*). In the latter species and other coastal temperate diatoms, mitochondrial respiration is used to produce additional ATP, which is needed for C fixation and cell metabolism (39). However, in *T. oceanica*, additional needed ATP has been hypothesized to be produced from a more iron-efficient PSII water–water cycle, in which photosynthetically produced electrons are used to reduce O_2 back to water downstream of PSII via the enzyme plastoquinol terminal oxidase (PTOX), which contains 2 Fe atoms (31). This process produces a hydrogen ion gradient across thylakoid membranes for ATP synthesis, but no net NADPH synthesis, and has been hypothesized (31, 40, 41) to account for the very high PSII:PSI ratios observed in this oceanic diatom (13) (Table 1). This PTOX-related process was not considered in our estimation of photosynthetic iron in *T. oceanica* (Table 1). If it were, and one PTOX was needed for every PSII complex used in this process [i.e., the PSII complexes in excess of those needed for linear PET, ~1.7 times the PSI complex concentration (9, 31)], then the photosynthetic Fe:C ratio in iron-limited *T. oceanica* would increase by 1.36-fold, and the estimated photosynthetic iron use efficiency would decrease by an equal relative amount, from 137 to 101 kmol C·(mol Fe)$^{-1}$·d^{-1}. This value is lower than the mean photosynthetic iron use efficiencies for the iron-limited SO species [120 ± 21 kmol C·(mol Fe)$^{-1}$·d^{-1}].

Other iron-saving adaptations include the replacement of the iron-containing photosynthetic electron carrier Cyt c_6 with the copper protein plastocyanin (42) and replacement of the iron-sulfur protein ferredoxin with the nonmetal protein flavodoxin (43). In iron-sufficient cultures, gene transcripts for both plastocyanin and flavodoxin were found in all nine of the SO diatoms examined (26), including our experimental species *E. antarctica*. By contrast, ferredoxin transcripts were detected in only five of the nine species, and these occurred at only low levels (26). However, these iron-replacement adaptations are not unique to the SO, as our temperate oceanic diatom *T. oceanica* also constitutively expresses plastocyanin under both high- and low-iron conditions (42) and flavodoxin largely replaces ferredoxin in low-iron cultures of *T. weissflogii* and *T. oceanica* (13).

Our findings suggest that SO phytoplankton have evolved critical mechanisms to economize on the use of iron and increase light absorption and specific rates of electron transport at low light intensities and low iron levels, which have allowed them to adapt to their cold, iron- and light-stressed environment. Of particular interest may be the role of low temperature in facilitating these adaptations, a hypothesis which warrants further investigation. These findings should help us to better understand and model the mechanisms that set the photosynthetic carbon fixation rate in the SO and its response to ongoing global warming and climate change. Our findings should also help to better predict the productivity of this vast ecosystem, and its impact on global carbon cycles, atmospheric CO_2, and global climate (2).

Materials and Methods

Study Organisms. Experiments were conducted with two diatoms (*P. inermis* and *E. antarctica*) and the haptophyte *P. antarctica* (clone AA1) isolated from the Southern Ocean south of the polar front (18, 19). *P. antarctica* did not form colonies during our experiments. For comparison, we also examined two temperate diatoms: *T. oceanica* [Center for Culture of Marine Phytoplankton (CCMP) 1003], an oceanic species from the Sargasso Sea, and the coastal species *T. weissflogii* (CCMP 1336), isolated from Long Island Sound, NY. Both were obtained from the Provasoli-Guillard National Center for Marine Algae and Microbiota.

Culturing. SO algal cultures were grown at 3 ± 1 °C in continuous light at an intensity of 30 μmol quanta·m^{-2}·s^{-1}, and temperate diatoms were grown at 18 ± 1 °C in continuous light at 40 μmol quanta·m^{-2}·s^{-1}. Light was provided from fluorescent bulbs (40-W Vita-Lite; Duro-Test) attenuated with neutral-density screening, and was measured with a 4π quantum sensor (model QSL-2100; Biospherical Instruments).

All experimental cultures were grown in triplicate. They were grown as semicontinuous batch cultures in trace metal ion buffered synthetic seawater medium (Aquil; pH 8.3) containing 10 μmol·L^{-1} EDTA using trace metal-clean techniques (18, 44). Calculated free trace metal ion concentrations were as follows: Cu, $10^{-14.07}$ M; Mn, $10^{-8.17}$ M; Zn, $10^{-10.79}$ M; and Co, $10^{-11.09}$ M. For the temperate diatoms, high- and low-iron media contained total iron concentrations of 58 and 4.4 nmol·L^{-1}, which correspond to computed concentrations of dissolved inorganic iron hydrolysis species ([Fe′]) of 1,400 and 104 pmol·L^{-1} (18, 19). Total iron concentrations included that added as filter-sterilized Fe-EDTA chelates plus a measured background concentration of 1.8 ± 0.1 nmol·L^{-1} (18). For the SO species, the high-iron medium contained 4.4 nmol·L^{-1} ([Fe′], 145 pmol·L^{-1} at 3 °C) (18, 45). To induce a comparable degree of iron limitation in the SO species, a single low-iron concentration was used (3.8 nmol·L^{-1}) along with different concentrations of the strong iron-binding siderophore desferrioxamine B (DFB; Sigma-Aldrich), which was added in addition to the EDTA. The following DFB concentrations were used: *P. antarctica*, 400 nmol·L^{-1} ([Fe′], 0.02 pmol·L^{-1}); *P. inermis*, 200 nmol·L^{-1} ([Fe′], 0.03 pmol·L^{-1}); and *E. antarctica*, 40 nmol·L^{-1} ([Fe′], 0.17 pmol·L^{-1}).

All phytoplankton species were maintained under axenic conditions (19). Growth rates of acclimated cells were determined from in vivo chlorophyll *a* fluorescence using a Turner Designs model 10-AU fluorometer. Specific growth rates (d^{-1}) were calculated from least-squares regressions of ln in vivo fluorescence versus time for exponentially growing cultures. All experimental cultures were grown for 14 to 16 generations before analytical measurements, and specific growth rates remained stable over the period of the study (19).

Biochemical Composition. Replicate (n = 3) 2-L (temperate diatoms) and 10-L (SO species) cultures were harvested, and cell concentration and average volume per cell were immediately measured on culture subsamples of *T. weissflogii*, *T. oceanica*, and *P. antarctica* with a calibrated Coulter counter (model Z2; Beckman Coulter) and by visual microscopy for *P. inermis* and *E. antarctica* as described previously (18, 19). Intracellular iron and cellular carbon concentrations were measured in parallel cultures grown in 28-mL polycarbonate tubes using the radiotracers [^{14}C]bicarbonate (specific activity 28 kBq; PerkinElmer) and $^{55}FeCl_3$ (specific activity 920 to 2,015 MBq·L^{-1}; PerkinElmer). For intracellular iron measurements, the cells were washed with a titanium(III) EDTA-citrate reducing solution to remove iron oxyhydroxides and ferric iron adsorbed to cell surfaces (19). Specific growth rates and F_v/F_m (see below) in small (28-mL) radiolabeled cultures and large (2-, 10-L) unlabeled cultures differed by less than 10 ± 1%, indicating comparable growth conditions between cultures. Oxygen flash yields and the reaction center of PSI, P700, were used as proxies for PSII and PSI, respectively. For these calculations, we assumed that P700 was present within functional complexes only, and in a fixed stoichiometry to the other subunits of PSI. P700 was measured by spectroscopy (46). Cell concentrates for P700 analyses were prepared by concentrating cells on 20-μm polycarbonate filters (Poretics) by gravity filtration for *P. inermis*, or by centrifugation [20,000 × *g*, 10 min, 3 °C (SO species) or 18 °C (temperate diatoms)] for the other species (three technical replicates per biological replicate). Oxygen flash yields (46) were performed to determine cellular PSII concentrations as described previously (13). The cellular concentrations of functional PSII and PSI were calculated from Chl *a*:PSII and Chl *a*:PSI ratios and cellular Chl *a* concentrations, which were measured fluorometrically (18).

Photosynthetic Measurements. Photosynthetic measurements [oxygen flash yields, photosynthesis-versus-irradiance curves, and fast repetition rate (FRR) fluorometry] were performed on samples acclimated in the dark for 30 min. A Chelsea Instruments FASTtracka FRR fluorometer was used to calculate the ratio of variable-to-maximum fluorescence (F_v/F_m, where $F_v = F_m - F_o$) and the functional absorption cross-section of PSII (σ_{PSII}) at 3 °C (SO species) or 18 °C (temperate species) using v6 data processing software (18). Cell concentrates (three technical replicates per biological replicate) were prepared for P–E and oxygen flash yield measurements by gravity filtration (*P. inermis*; 20-μm polycarbonate membrane filters) or centrifugation (other species; 20,000 × *g*, 4 min) and resuspending the cells in 0.2-μm filter-sterilized growth medium. P–E curves were determined at 18 °C (temperate species) or 3 °C (SO species) using a calibrated oxygen electrode system (Hansatech; model DW1), quartz-halogen light source, and neutral-density filters. Changes in O_2 concentration were measured at 14 irradiances (3 min per irradiance) ranging from 0 to 2,665 μmol quanta·m^{-2}·s^{-1}, and an exponential function (47) was fitted to the P–E data. The maximum rate at which electrons can be transferred from water to CO_2 in the steady state (1/τ; ms^{-1}) was calculated as follows: $1/\tau = P^B_{max}/n$, where P^B_{max} is the maximum

ENVIRONMENTAL SCIENCES

photosynthetic rate normalized to Chl *a*, and *n* is the oxygen flash yield (mol O_2·mol^{-1} Chl *a*) (48).

Statistical Analyses. Biological replicate means and SEM were calculated using Microsoft Excel software (version 2017 for Mac). Data were examined for normality and equal variance before two-way ANOVA and Tukey's (species effects) and Bonferroni's (iron effects) post hoc multiple comparison tests (Prism 6 for Mac; GraphPad Software). Significant results are reported at the 95% confidence level ($P < 0.05$). Linear regression analyses were performed using Prism 6.

ACKNOWLEDGMENTS. We thank Maria Maldonado, Philippe Tortell, Beverley Green, and Julian Eaton-Rye for providing laboratory facilities, and Sam Laney for providing the v6 code for fast repetition rate fluorometry data processing. Funding for this work was provided by grants from the Marsden Fund of New Zealand and the Ministry of Science and Innovation New Zealand.

1. Field CB, Behrenfeld MJ, Randerson JT, Falkowski P (1998) Primary production of the biosphere: Integrating terrestrial and oceanic components. *Science* 281:237–240.
2. Marinov I, Gnanadesikan A, Toggweiler JR, Sarmiento JL (2006) The Southern Ocean biogeochemical divide. *Nature* 441:964–967.
3. Moore CM, et al. (2013) Processes and patterns of oceanic nutrient limitation. *Nat Geosci* 6:701–710.
4. Boyd PW (2002) Environmental factors controlling phytoplankton processes in the Southern Ocean. *J Phycol* 38:844–861.
5. Boyd PW, et al. (2007) Mesoscale iron enrichment experiments 1993-2005: Synthesis and future directions. *Science* 315:612–617.
6. Hunt GL, Jr, et al. (2016) Advection in polar and sub-polar environments: Impacts on high latitude marine ecosystems. *Prog Oceanogr* 149:40–81.
7. Constable AJ, et al. (2014) Climate change and Southern Ocean ecosystems I: How changes in physical habitats directly affect marine biota. *Glob Change Biol* 20: 3004–3025.
8. Malviya S, et al. (2016) Insights into global diatom distribution and diversity in the world's ocean. *Proc Natl Acad Sci USA* 113:E1516–E1525.
9. Suggett DJ, Le Floc'h E, Harris GN, Leonardos N, Geider RJ (2007) Different strategies of photoacclimation by two strains of *Emiliania huxleyi* (Haptophyta). *J Phycol* 43: 1209–1222.
10. Raven JA (1990) Predictions of Mn and Fe use efficiencies of phototrophic growth as a function of light availability for growth and of C assimilation pathway. *New Phytol* 116:1–18.
11. Sunda WG, Huntsman SA (1997) Interrelated influence of iron, light, and cell size on marine phytoplankton growth. *Nature* 390:389–392.
12. Sunda WG, Huntsman SA (2011) Interactive effects of light and temperature on iron limitation in a marine diatom: Implications for marine productivity and carbon cycling. *Limnol Oceanogr* 56:1475–1488.
13. Strzepek RF, Harrison PJ (2004) Photosynthetic architecture differs in coastal and oceanic diatoms. *Nature* 431:689–692.
14. Falkowski PG, Raven JA (2007) *Aquatic Photosynthesis* (Princeton Univ Press, Princeton, NJ).
15. Lavergne J, Joliot P (2000) Thermodynamics of the excited states of photosynthesis. *Biophysics Textbook OnLine*, ed Cramer WA (Biophys Soc, Bethesda), pp 1–12.
16. Suggett DJ, Moore CM, Hickman AE, Geider RJ (2009) Interpretation of fast repetition rate (FRR) fluorescence: Signatures of phytoplankton community structure versus physiological state. *Mar Ecol Prog Ser* 376:1–19.
17. Wientjes E, van Amerongen H, Croce R (2013) Quantum yield of charge separation in photosystem II: Functional effect of changes in the antenna size upon light acclimation. *J Phys Chem B* 117:11200–11208.
18. Strzepek RF, Hunter KA, Frew RD, Harrison PJ, Boyd PW (2012) Iron–light interactions differ in Southern Ocean phytoplankton. *Limnol Oceanogr* 57:1182–1200.
19. Strzepek RF, Maldonado MT, Hunter KA, Frew RD, Boyd PW (2011) Adaptive strategies by Southern Ocean phytoplankton to lessen iron limitation: Uptake of organically complexed iron and reduced cellular iron requirements. *Limnol Oceanogr* 56: 1983–2002.
20. Greene RM, Geider RJ, Falkowski PG (1991) Effect of iron limitation on photosynthesis in a marine diatom. *Limnol Oceanogr* 36:1772–1782.
21. Hiscock MR, et al. (2008) Photosynthetic maximum quantum yield increases are an essential component of the Southern Ocean phytoplankton response to iron. *Proc Natl Acad Sci USA* 105:4775–4780.
22. Alderkamp A-C, et al. (2012) The effect of iron limitation on the photophysiology of *Phaeocystis antarctica* (Prymnesiophyceae) and *Fragilariopsis cylindrus* (Bacillariophyceae) under dynamic irradiance. *J Phycol* 48:45–59.
23. Ryan-Keogh TJ, Thomalla SJ, Little H, Melanson JR (2018) Seasonal regulation of the coupling between photosynthetic electron transport and carbon fixation in the Southern Ocean. *Limnol Oceanogr* 63:1856–1876.
24. Halsey KH, Jones BM (2015) Phytoplankton strategies for photosynthetic energy allocation. *Annu Rev Mar Sci* 7:265–297.
25. Fisher NL, Halsey KH (2016) Mechanisms that increase the growth efficiency of diatoms in low light. *Photosynth Res* 129:183–197.
26. Moreno CM, et al. (2018) Examination of gene repertoires and physiological responses to iron and light limitation in Southern Ocean diatoms. *Polar Biol* 41:679–696.
27. Brand LE, Sunda WG, Guillard RRL (1983) Limitation of marine phytoplankton reproductive rates by zinc, manganese, and iron. *Limnol Oceanogr* 28:1182–1198.
28. Sunda WG, Huntsman SA (1995) Iron uptake and growth limitation in oceanic and coastal phytoplankton. *Mar Chem* 50:189–206.
29. Raven JA (2006) The role for vacuoles. *New Phytol* 106:357–422.
30. Ryan-Keogh TJ, et al. (2016) Temporal progression of photosynthetic-strategy in phytoplankton in the Ross Sea, Antarctica. *J Mar Syst* 166:87–96.
31. Behrenfeld MJ, Milligan AJ (2013) Photophysiological expressions of iron stress in phytoplankton. *Annu Rev Mar Sci* 5:217–246.
32. Macey AI, Ryan-Keogh T, Richier S, Moore CM, Bibby TS (2014) Photosynthetic protein stoichiometry and photophysiology in the high latitude North Atlantic. *Limnol Oceanogr* 59:1853–1864.
33. Morgan-Kiss RM, Priscu JC, Pocock T, Gudynaite-Savitch L, Huner NPA (2006) Adaptation and acclimation of photosynthetic microorganisms to permanently cold environments. *Microbiol Mol Biol Rev* 70:222–252.
34. Marchetti A, Catlett D, Hopkinson BM, Ellis K, Cassar N (2015) Marine diatom proteorhodopsins and their potential role in coping with low iron availability. *ISME J* 9: 2745–2748.
35. Cohen NR, et al. (2017) Diatom transcriptional and physiological responses to changes in iron bioavailability across ocean provinces. *Front Mar Sci* 14:360.
36. Marchetti A, et al. (2012) Comparative metatranscriptomics identifies molecular bases for the physiological responses of phytoplankton to varying iron availability. *Proc Natl Acad Sci USA* 109:E317–E325.
37. Dioumaev AK, et al. (2002) Proton transfers in the photochemical reaction cycle of proteorhodopsin. *Biochemistry* 41:5348–5358.
38. Kloer DP, Ruch S, Al-Babili S, Beyer P, Schulz GE (2005) The structure of a retinal-forming carotenoid oxygenase. *Science* 308:267–269.
39. Bailleul B, et al. (2015) Energetic coupling between plastids and mitochondria drives CO_2 assimilation in diatoms. *Nature* 524:366–369.
40. Behrenfeld MJ, Halsey KH, Milligan AJ (2008) Evolved physiological responses of phytoplankton to their integrated growth environment. *Philos Trans R Soc Lond B Biol Sci* 363:2687–2703.
41. Mackey KRM, Paytan A, Grossman AR, Bailey S (2008) A photosynthetic strategy for coping in a high-light, low-nutrient environment. *Limnol Oceanogr* 53:900–909.
42. Peers G, Price NM (2006) Copper-containing plastocyanin used for electron transport by an oceanic diatom. *Nature* 441:341–344.
43. La Roche J, Boyd PW, McKay ML, Geider RJ (1996) Flavodoxin as an in situ marker for iron stress in phytoplankton. *Nature* 382:802–805.
44. Maldonado MT, Price NM (1996) Influence of N substrate on Fe requirements of marine centric diatoms. *Mar Ecol Prog Ser* 141:161–172.
45. Sunda WG, Huntsman SA (2003) Effect of pH, light, and temperature on Fe-EDTA chelation and Fe hydrolysis in seawater. *Mar Chem* 84:35–47.
46. Falkowski PG, Owens TG, Ley AC, Mauzerall DC (1981) Effects of growth irradiance levels on the ratio of reaction centers in two species of marine phytoplankton. *Plant Physiol* 68:969–973.
47. Platt T, Gallegos CL, Harrison WG (1980) Photoinhibition of photosynthesis in natural assemblages of marine phytoplankton. *J Mar Res* 28:687–701.
48. Ley AC, Mauzerall DC (1982) Absolute absorption cross-sections for photosystem II and the minimum quantum requirement for photosynthesis in *Chlorella vulgaris*. *Biochim Biophys Acta* 680:95–106.